Progress In Electromagnetics Research C, Vol. 32, 221–232, 2012

DESIGN OF DUAL-BAND BANDPASS FILTER WITH WIDE UPPER STOPBAND USING SIR AND GSIR STRUCTURES

M. Mashhadi* **and N. Komjani**

College of Electrical Engineering, Iran University of Science and Technology, Narmak, Tehran, Iran

Abstract—In this paper, a new dual-band bandpass (BPF) filter with multi-spurious suppression is proposed, which is composed of step-impedance resonators (SIR) and grounded-step-impedance resonators (GSIR). It is shown that the resonant frequencies of GSIR can be obtained similar to SIR. Then, by determining the dimensions of SIR to have a specified resonant frequencies ratio, the dimensions of GSIR can be calculated. It is also shown that the coupling lengths between SIR and GSIR can create several transmissions zeros and can be used to suppress the unwanted higher order resonant frequencies. A third-order filter is designed and fabricated to operate at two WLAN frequencies of 2.45 GHz and 5.8 GHz. The measured results show a rejection level of 24 dB up to more than 17 GHz ($7f_1$). Simulation and measurement results are in good agreement with each other.

1. INTRODUCTION

Recently, dual-band or multi-band bandpass filters (BPF) have gained much attention in the context of modern wireless communication applications such as wireless local area networks (WLANs). So far, different approaches have been introduced for the design dual-band BPFs [1–10]. In [1, 2], by connecting two different BPFs in parallel, the dual-band BPF was designed. Complicated frequency transformation technique has been used in [3] to design a dual-band BPF. Another well-known method used to the design of dual-band BPFs is using SIR [4, 7]. In [8, 9], slotted ground structures were utilized to design a dual-band BPF. Adding inner stubs to resonator was another method used

Received 31 July 2012, Accepted 13 September 2012, Scheduled 18 September 2012

* Corresponding author: Mostafa Mashhadi (mashhadi@elec.iust.ac.ir).

to design dual-band BPF [10, 11]. In [12], the meandered technology and the fractal geometry were used to design a compact dual-band BPF.

However, all these dual-band BPFs discussed above suffer from unwanted higher resonant frequencies which limit the bandwidth of the upper stopband. So far, various techniques have been proposed to design a dual-band BPF with a wide upper stopband [13–15]. In [13], suppression of spurious frequencies was realized by using SIRs with different dimensions. The SIRs were designed to have two identical resonant frequencies at two passbands, but the higher order resonant frequencies of SIRs are different. The over-coupled structure was used in [14] to suppress the unwanted spurious resonance frequencies. In [15], stub-loaded SIR was used to design a dual-band BPF with a wide upper stopband. Suppression of spurious frequencies in this filter was achieved using stub-loaded section.

In this paper, a novel dual-band BPF with a wide upper stopband using SIR and GSIR is proposed. The coupling length between SIR and GSIR can create several transmissions zeros that are used to suppress the unwanted resonance frequencies.

2. RESONANT FREQUENCIES OF SIR AND GSIR

2.1. SIR

The resonant frequencies of a SIR which is shown in Fig. 1(a) can be obtained by the following equations [16].

$$\tan\theta_1 \cdot \tan\theta_2 = K\,, \quad \text{odd mode} \tag{1}$$

$$\tan\theta_2 = -K\tan\theta_1\,, \quad \text{even mode} \tag{2}$$

where $K = Z_2/Z_1$, θ_1 and θ_2 are electrical lengths of the microstrip lines with characteristic impedances Z_1 and Z_2, respectively. The resonant frequencies of f_2 through f_5 are normalized to the fundamental frequency f_1 and plotted as a function of α in Fig. 1(b), where α is defined as $\theta_2/(\theta_1+\theta_2)$. It can be observed that by decreasing K, the ratios of f_2/f_1, f_3/f_1, f_4/f_1 and f_5/f_1 increases.

As seen in Fig. 1(b), there are two arbitrary parameters α and K that change the resonant frequencies ratios. Therefore, for a specific resonant frequencies ratio of f_2/f_1, different values of α and K can be chosen. For example, if SIR is designed so that its first two resonant frequencies are 2.45 GHz and 5.8 GHz ($f_2/f_1 = 2.367$), it can be shown from (1) and (2) that the values of α and K are related to each other by Fig. 2(a). It can be observed that K must be less than 0.68, so that the specific resonance ratio of 2.367 is obtained. It is also seen that two values of K may exist for a specified α. For selecting the optimum

values of α and K, the length of resonator and also the normalized resonant frequencies must be determined as a functions of α or K. In this paper, a filter is designed on a substrate with a relative dielectric constant of 3.55 and thickness of 0.813 mm. For this substrate, the lengths of low and high impedance lines and also the total length of resonator versus α are shown in Fig. 2(b) while f_1 and f_2 are 2.45 GHz and 5.8 GHz, respectively. It is observed that by decreasing α, the length of resonator is also decreased. Fig. 3 shows the resonant frequencies and the ratios of high order resonant frequencies to first resonant frequency as a function of α. It is observed that by decreasing α, the unwanted resonant frequencies increase. Therefore, the value of α should be chosen as small as possible in order to decrease the length of resonator and also push the unwanted resonant frequencies to the higher frequency region. It is also noticed that α cannot be selected so small since it causes a small value of K. This small value of K makes a very large discontinuity and creates radiation losses in the high frequency responses of filter.

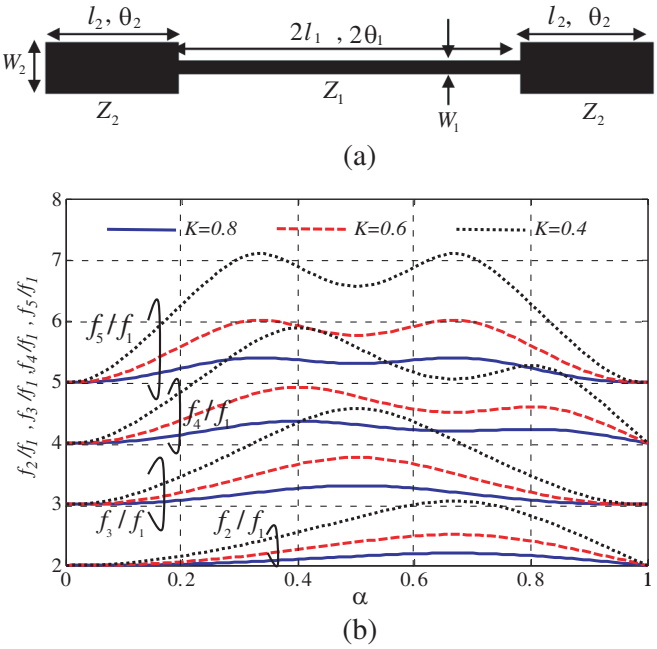

Figure 1. (a) Stepped-impedance resonator structure. (b) The ratio of higher resonant frequencies to fundamental resonant frequency for different values of K.

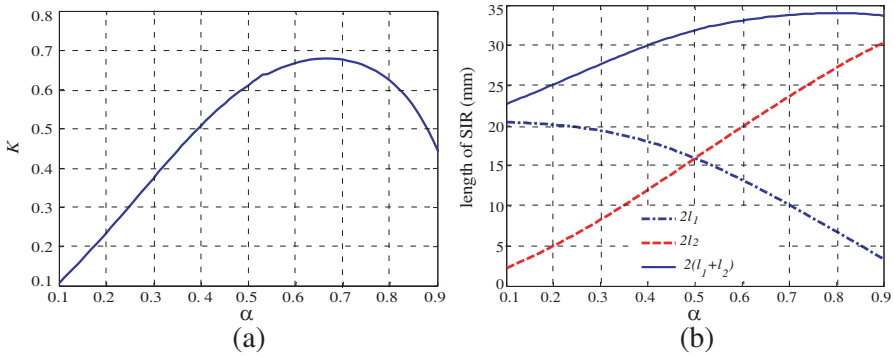

Figure 2. (a) Relation between α and K in order to have $f_2/f_1 = 2.367$. (b) The lengths of low and high impedance lines and also the total length of resonator in order to have $f_1 = 2.45\,\text{GHz}$ and $f_2 = 5.8\,\text{GHz}$.

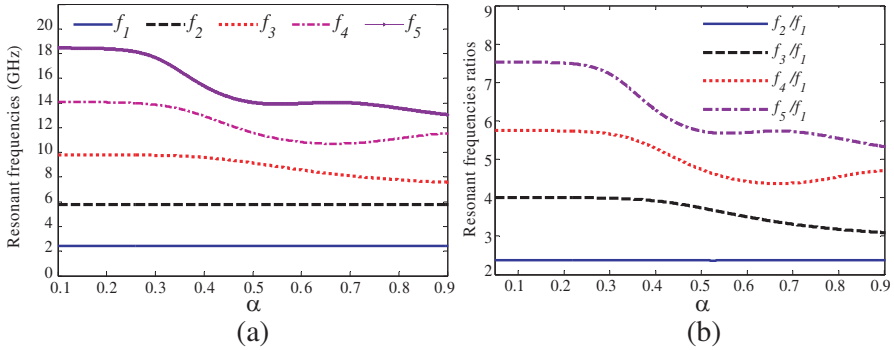

Figure 3. (a) The resonant frequencies versus α while f_1 and f_2 are fixed. (b) The ratios of high order resonant frequencies to first resonant frequency versus α while f_1 and f_2 are fixed.

2.2. GSIR

The configuration of GSIR is shown in Fig. 4. The resonant frequencies of this structure can be calculated by odd and even mode analysis. The odd and even mode equivalent circuits of GSIR are shown in Figs. 5(a) and (b), respectively. In GSIR, since two ends of the resonator are connected to the ground, the structure is resonant when its input impedance is zero for the even or odd modes.

It can be easily shown that the resonant frequencies of odd mode equivalent circuit is

$$Z_{2,g} \tan\theta_{2,g} = -Z_{1,g} \tan\theta_{1,g} \tag{3}$$

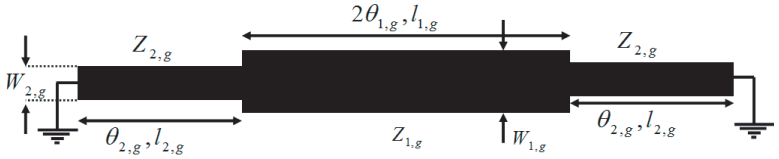

Figure 4. Schematic of grounded-stepped-impedance resonator (GSIR).

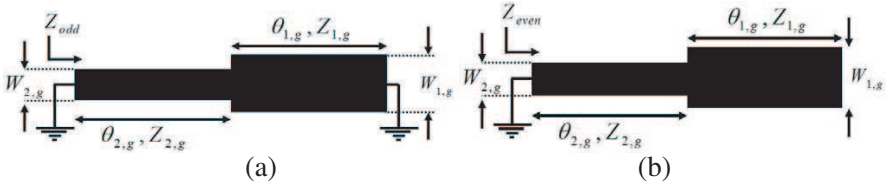

Figure 5. Equivalent circuit of GSIR. (a) Odd-mode equivalent circuit. (b) Even-mode equivalent circuit.

where $\theta_{1,g}$ and $\theta_{2,g}$ are electrical lengths of the microstrip lines with characteristic impedances $Z_{1,g}$ and $Z_{2,g}$, respectively. If we define $K' = Z_{2,g}/Z_{1,g}$, (3) can be expressed as

$$\tan\theta_{2,g} = -\frac{1}{K'}\tan\theta_{1,g} \tag{4}$$

This equation is similar to (2) in which K is converted to $K = 1/K'$. In other words, from (2) and (4) it can be concluded that the odd mode resonant frequencies of GSIR are equal to the even mode resonant frequencies of SIR with the same electrical length and reversed impedance ratio ($K = 1/K'$).

The input impedance of even mode equivalent circuit of GSIR is

$$Z_{even} = jZ_{2,g}\frac{-Z_{1,g}\cot\theta_{1,g} + Z_{2,g}\tan\theta_{2,g}}{Z_{2,g} + Z_{1,g}\cot\theta_{1,g}\tan\theta_{2,g}} \tag{5}$$

Therefore, the even mode resonant frequencies of GSIR can be expressed as

$$\tan\theta_{1,g}\tan\theta_{2,g} = \frac{1}{K'} \tag{6}$$

By comparing (1) and (6), we can conclude that the even mode resonant frequencies of GSIR are equal to odd mode resonant frequencies of SIR with the same electrical length and reversed impedance ratio ($K = 1/K'$).

Generally, from (4) and (6) we conclude that the resonant frequencies of GSIR can be obtained by using of corresponding SIR. In

fact, if the impedance ratio of a SIR structure is equal to $K = 1/K'$, then the resonant frequencies of GSIR and SIR are the same so that the even and odd mode resonant frequencies of GSIR are equal to odd and even mode resonant frequencies of SIR, respectively. Therefore, for analyzing and designing of GSIR structure, first, the SIR structure can be analyzed and designed, then the desired GSIR has the same electrical length with designed SIR and its impedance ratio is reverse of impedance ratio of SIR.

3. FILTER DESIGN PROCEDURE

By using SIR and GSIR structures, a third order dual-band BPF is designed. The schematic of proposed filter is shown in Fig. 6. The filter is composed of two SIR and one GSIR structure. Two resonators are designed so that first two resonant frequencies of them are the same but have different spurious resonant frequencies to make spurious peaks have low levels and small bandwidths. After design and optimizations, the dimensions of SIR and GSIR structures are adopted as $W_1 = 0.4\,\text{mm}$, $W_2 = 1.3\,\text{mm}$, $l_1 = 9\,\text{mm}$, $l_2 = 7\,\text{mm}$, $W_{1,g} = 1.7\,\text{mm}$, $W_{2,g} = 0.4\,\text{mm}$, $l_{1.g} = 8.2\,\text{mm}$, $l_{2,g} = 6\,\text{mm}$, $W_{pad} = 2\,\text{mm}$, $D = 0.8\,\text{mm}$. The first six resonant frequencies of SIR and GSIR are also shown in Table 1.

After determining the dimensions of SIR and GSIR resonators, the coupling structure between resonators must be designed. In [17], it is shown that the coupling lengths between open-ended and short-

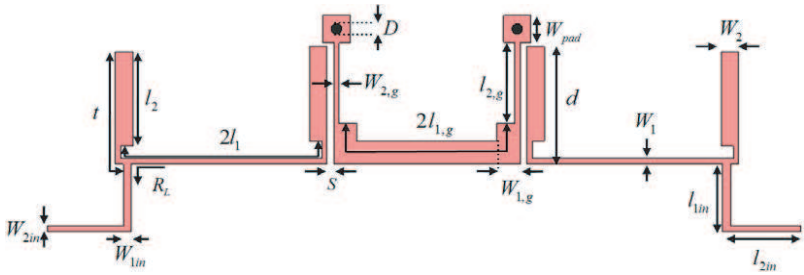

Figure 6. The schematic of proposed filter.

Table 1. The first six resonant frequencies of resonators.

Resonant frequencies (GHz)	f_1	f_2	f_3	f_4	f_5	f_6
SIR	2.45	5.8	9.15	11.6	14.1	17.6
GSIR	2.45	5.8	10.3	12.9	14.5	18.1

ended resonators can be adopted such that create transmission zeros and suppress unwanted resonant frequencies. This technique is used in the proposed filter to suppress the spurious resonant frequencies. In the proposed filter, because GSIR is located between two SIRs and because SIRs are directly connected to feed lines, the unwanted resonances of SIR are suppressed more than the GSIR ones. Hence, the length of coupling structure is determined so to suppresses the unwanted resonances of GSIR. The schematic of coupling structure and its frequency responses for different values of d are shown in Figs. 7(a) and (b), respectively. It is observed that coupling structure can create several transmission zeros, and by increasing the coupling length, the transmission zeros are decreased. If $d = 8.7\,\text{mm}$ is adopted, the transmission zeros of coupling structure will be at frequencies of 10.8, 12.8 and 18 GHz which are in the vicinity of resonant frequencies of f_3, f_4 and f_6 of GSIR, respectively. Therefore, by selecting this length of coupling the resonances of f_3, f_4 and f_6 of GSIR are suppressed.

Another way to create transmission zeros is to apply the tapped input and output structure [18]. It is shown that these transmission zeros can be tuned by sliding the tap position along the end resonators. The zeros created by the tapped input/output are plotted as a function of t in Fig. 8. The zeros occur at the frequencies where t is equivalent to a $\lambda/4$ or $3\lambda/4$ — section uniform line. It is observed that when t changes between 7–15 mm, the tapped input/output creates two transmission zeros in the range of 2–20 GHz. One of the transmission zeros occurs between two passband and therefore increases isolation between two passbands. The other transmission zero can be used to suppress the spurious resonances. If $t = 9.2\,\text{mm}$ is adopted, the second

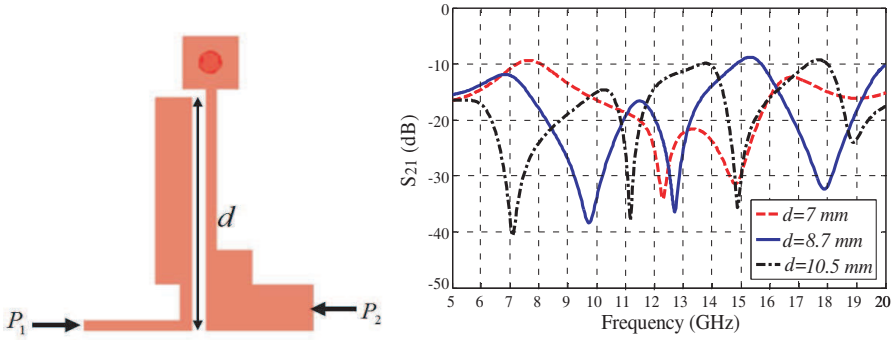

Figure 7. (a) Schematic of coupling structure. (b) Frequency responses of coupling structure for various d.

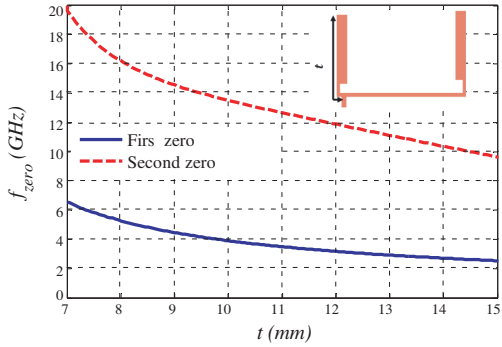

Figure 8. The transmission zeros of tapped input/output structure.

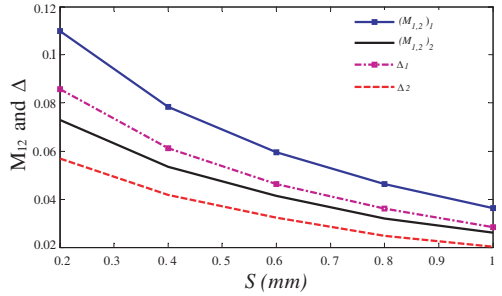

Figure 9. The coupling coefficient and fractional bandwidth between resonators at two passbands versus S.

transmission zero of tapped structure suppresses the resonance of GSIR structure at f_5.

In the proposed filter, it is supposed that ripples for both passbands are 0.01 dB. As shown in [15], the fractional bandwidth between coupled resonators can be obtained by following equation.

$$\Delta_j = (M_{1,2})_j \sqrt{g_{1,j} g_{2,j}} \tag{7}$$

$(M_{1,2})_j$ is the coupling coefficient between first and second resonators at jth passband which is obtained by simulation. $g_{i,j}$ represents the ith element value of the lowpass prototype filter at the jth passband, $g_{0,1}$=$g_{0,2}$= 1, $g_{1,1}$=$g_{3,1}$=$g_{1,2}$=$g_{3,2}$= 0.6292 and $g_{2,1}$=$g_{2,2}$= 0.9703 for the Chebyschev filter. The coupling coefficient and fractional bandwidth between SIR and GSIR at two passbands versus S are plotted in Fig. 9. According to Fig. 9, when S changes between 0.2–1 mm, the fractional bandwidths for the first passband are from 2.8% to 8.6%, and for the second passband from 2% to 5.7%. By selecting $S = 0.5$ mm, the fractional bandwidths at two passbands are equal to 5.7% and 3.7%, respectively.

The last step to complete the design of dual-band BPF is to determine the dual-band impedance transformer. According to [15], the load impedance seen at the tap point toward the input/output port at the jth passband which is also shown in Fig. 6 is calculated by the following equation.

$$R_{L,j} = \frac{2g_{0,j}g_{1,j}}{\Delta_j f_j}\left(\frac{\partial B(f)}{\partial f}\bigg|_{f=f_j}\right)^{-1} \tag{8}$$

where B is total susceptance of the resonator obtained by simulation. For $t = 9.2\,\text{mm}$, the load impedances at the first and second passbands are $220\,\Omega$ and $45\,\Omega$, respectively. Then the parameters of l_{1in}, W_{1in}, l_{2in} and W_{2in} are obtained using optimization to provide the required load impedances at two passbands and results in $l_{1in} = 5\,\text{mm}$, $W_{1in} = 0.6\,\text{mm}$, $l_{2in} = 11.5\,\text{mm}$, $W_{2in} = 0.4\,\text{mm}$.

4. SIMULATION AND MEASUREMENT

The schematic of the fabricated filter is shown in Fig. 10. The dual-band BPF is simulated using CST Microwave Studio. The simulated and measured frequency responses of filter are shown in Fig. 11. It is seen that the spurious resonances are effectively suppressed with rejection more than 24 dB and 20 dB up to $7f_1$ (17 GHz) and $7.7f_1$ (18.5 GHz), respectively. The measured insertion losses at f_1 and f_2 are 1.54 dB and 2.25 dB, respectively and return losses in both passbands are better than 20 dB. The frequency responses of the filter at two passbands are shown in Fig. 12. It is observed that there are very good agreements between simulated and measured results at the two passbands. This filter also shows some radiation loss in high frequencies mainly caused by discontinuities of SIR and GSIR structures which can limit the application of the filter.

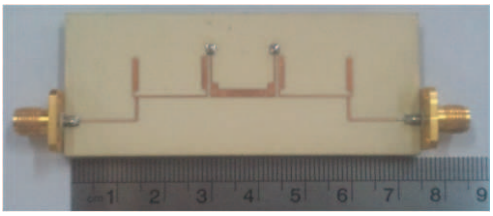

Figure 10. Photograph of the manufactured filter.

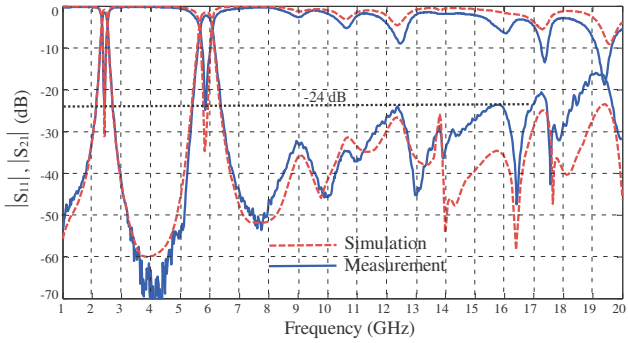

Figure 11. Simulated and measured frequency responses of dual-band BPF.

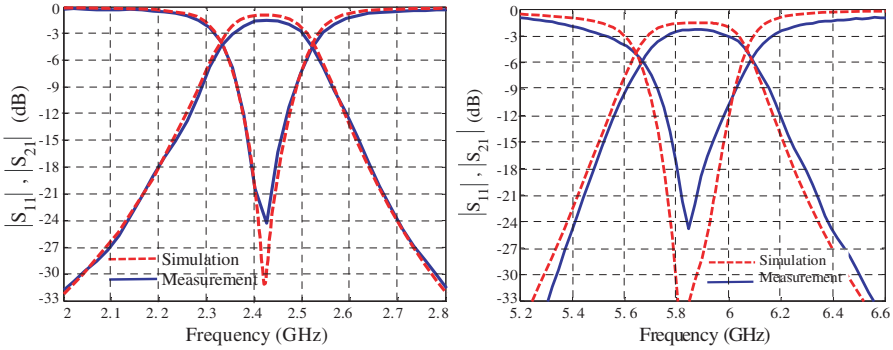

Figure 12. Simulated and measured frequency responses of dual-band BPF at two passbands.

5. CONCLUSION

In this paper, a new approach to design a dual-band BPF with a wide upper stopband has been presented. Firstly, the resonant frequencies of SIR and GSIR are obtained, and it is shown that the design of GSIR structure can be done similar to SIR structure. Then using these two resonators, a dual-band BPF with a wide upper stopband is designed. In the proposed filter, several techniques have been used to achieve a wide upper stopband. SIR and GSIR are designed to have different spurious resonant frequencies. It is also shown that the coupling structure between SIR and GSIR can create several transmission zeros which enhance the filter performance in the stopband. Another way to create transmission zeros is using tapped input/output structure. By properly selecting tap position, the created transmission zeros can

suppress the unwanted resonances. The dual-band BPF is fabricated to demonstrate the proposed ideas. The measured results agree well with the simulated ones, and a rejection better than 24 dB can be obtained up to more than $7f_1$.

ACKNOWLEDGMENT

This work was supported in part by the Iran Telecommunication Research Center.

REFERENCES

1. Abu-Hundrouss, A. M. and M. J. Lancaster, "Design of multiple-band microwave filters using cascaded filter elements," *Journal of Electromagnetic Waves and Applications*, Vol. 23, No. 16, 2109–2118, 2009.
2. Liang, F., B. Luo, W. Lu, and X. Wang, "A compact dual-band filter with close passbands using asymmetric $\lambda/4$ resonator pairs with shared via-hole ground," *Journal of Electromagnetic Waves and Applications*, Vol. 25, Nos. 8–9, 1289–1296, 2011.
3. Guan, X., Z. Ma, P. Cai, Y. Kobayashi, T. Anada, and G. Hagiwara, "Synthesis of dual-band bandpass filters using successive frequency transformations and circuit conversions," *IEEE Microw. Wireless Compon. Lett.*, Vol. 16, No. 3, 110–112, March 2006.
4. Alkanhal, M. A. S., "Dual-band bandpass filters using inverted stepped-impedance resonators," *Journal of Electromagnetic Waves and Applications*, Vol. 23, Nos. 8–9, 1211–1220, 2009.
5. Chu, Q.-X. and F.-C. Chen, "A compact dual-band bandpass filter using meandering stepped impedance resonators," *IEEE Microw. Wireless Compon. Lett.*, Vol. 18, No. 5, 320–322, May 2008.
6. Weng, M.-H., C.-H. Kao, and Y.-C. Chang, "A compact dual-band bandpass filter using cross coupled asymmetric SIRs for WLANs," *Journal of Electromagnetic Waves and Applications*, Vol. 24, Nos. 2–3, 161–168, 2010.
7. Lee, C.-H., I.-C. Wang, and C.-I. G. Hsu, "Dual-band balanced BPF using quarter wavelength stepped-impedance resonators and folded feed lines," *Journal of Electromagnetic Waves and Applications*, Vol. 23, Nos. 17–18, 2441–2449, 2009.
8. Wang, X.-H., B.-Z. Wang, and K. J. Chen, "Compact broadband dual-band bandpass filters using slotted ground structures," *Progress In Electromagnetics Research*, Vol. 82, 151–166, 2008.

9. Wang, J. P., B.-Z. Wang, Y. X. Wang, and Y.-X. Guo, "Dual-band microstrip stepped-impedance bandpass filter with defected ground structure," *Journal of Electromagnetic Waves and Applications*, Vol. 22, No. 4, 463–470, 2008.
10. Chen, F. C. and Q. X. Chu, "Novel multi stub loaded resonator and its application to high-order dual-band filters," *IEEE Trans. Microw. Theory and Tech.*, Vol. 58, 1551–1556, 2010.
11. Velazquez-Ahumada, M. D. C., J. Martel-Villagr, F. Medina, and F. Mesa, "Application of stub loaded folded stepped impedance resonators to dual band filters," *Progress In Electromagnetics Research*, Vol. 102, 107–124, 2010.
12. Chen, C.-Y. and C.-C. Lin, "The design and fabrication of a highly compact microstrip dual-band bandpass filter," *Progress In Electromagnetics Research*, Vol. 112, 299–307, 2011.
13. Kuo, J.-T. and H.-P. Lin, "Dual-band bandpass filter with improved performance in extended upper rejection band," *IEEE Trans. Microw. Theory Tech.*, Vol. 57, No. 4, 824–829, April 2009.
14. Jiang, M., L.-M. Chang, and A. Chin, "Design of dual-passband microstrip bandpass filters with multi-spurious suppression," *IEEE Microw. Wireless Compon. Lett.*, Vol. 20, No. 4, 199–201, April 2010.
15. Mashhadi, M. and N. komjani, "Design of novel dual-band bandpass filter with multi-spurious suppression for WLAN application," *Journal of Electromagnetic Waves and Applications*, Vol. 26, No. 7, 851–862, 2012.
16. Weng, M.-H., H.-W. Wu, and Y.-K. Su, "Compact and low loss dual-band bandpass filter using pseudo-interdigital stepped impedance resonators for WLANs," *IEEE Microw. Wireless Compon. Lett.*, Vol. 17, No. 3, 187–189, March 2007.
17. Dai, G. L., X. Y. Zhang, C. H. Chan, Q. Xue, and M. Y. Xia, "An investigation of open- and short-ended resonators and their applications to bandpass filters," *IEEE Trans. Microw. Theory and Tech.*, Vol. 57, No. 9, 2203–2210, September 2009.
18. Kuo, J.-T. and E. Shih, "Microstrip stepped-impedance resonator bandpass filter with an extended optimal rejection bandwidth," *IEEE Trans. Microw. Theory and Tech.*, Vol. 51, No. 5, 1554–1559, May 2003.